

Microstructural characteristics and paint-bake response of Al-Mg-Si-Cu alloy

Ji Yan-li(纪艳丽), GUO Fu-an(郭富安), PAN Yan-feng(潘琰峰)

Suzhou Institute for Nonferrous Metals Research, Suzhou 215026, China

Received 4 January 2007; accepted 17 October 2007

Abstract: The microstructural characteristics and paint-bake response of 6022 alloy with 0.3% Cu (mass fraction) were studied using optical microscope, scanning electron microscope(SEM), transmission electron microscope(TEM) and tensile tester. The results indicate that the phase constituents in the as-cast microstructure are Mg_2Si , Si, $Al_5Cu_2Mg_8Si_6$, Al_3FeSi , $\alpha-Al(MnCrFe)Si$ and $CuAl_2$. During the following homogenization, $CuAl_2$, $Al_5Cu_2Mg_8Si_6$ and Mg_2Si phases are almost completely dissolved, and Al_3FeSi transforms to $\alpha-Al(MnCrFe)Si$ particles. After rolling, the phase constituents in the alloy change less except the precipitation of Mg_2Si particles, and the precipitation behavior of Mg_2Si strongly depends on the thermomechanical conditions. Cu addition significantly increases the paint-bake response of 6022 alloy by facilitating the formation of β'' phase. Therefore, the tensile strength of 6022 alloy with 0.3% Cu is higher than that of 6022 alloy without Cu after paint-bake cycle.

Key words: Al-Mg-Si-Cu alloy; paint-bake response; Cu; β'' phase

1 Introduction

The heat treatable 6xxx (Al-Mg-Si) series aluminum alloys have received considerable interests from the automotive industry as potential autobody sheet material due to their ability to be shaped in the solution treated state and then age hardened during the paint bake cycle[1–3]. The main alloys of interest are AA6022, which has reasonable strength and high formability[4], and AA6111, which has high final strength[3]. The product route of automotive sheet can be divided into three stages[2]: 1) the breakdown of cast ingot to solutionised thin sheet via thermomechanical processing, 2) shaping of the product and 3) age hardening of the final product at temperatures of approximately 150–200 °C. The microstructure/precipitation response during stage 3 has been relatively well studied[3, 5–7]. The general accepted precipitation sequence during aging is as the following[7–8]: SSSS atomic clusters $\rightarrow \beta'' \rightarrow \beta' \rightarrow \beta$, where, SSSS is super saturated solid solution. Because of the short duration and low temperature of the automotive paint bake cycle, the alloy is under-aged and the main strengthening phase is β'' [3]. And Cu is often added to enhance the paint bake response[9–10].

In comparison, the microstructure evolution during

stage 1 has received much less attention though its impact is critical for achieving successful stage 2. ENGLER and HIRSCH[1] suggested that the control of the state of β precipitation during the entire chain of thermomechanical processing is the key factor to achieve a good formability and final surface appearance. And GUPTA et al[11] proposed that the precipitation process and the aging kinetics of strengthening phase are dependent on both the composition and the processing conditions. Therefore, the objective of the present work is to investigate precipitation state of Mg_2Si and Cu containing phases in AA6022 alloy with 0.3% Cu during the processing such as casting, homogenization, hot rolling and especially paint-bake cycle in order to develop a wider understanding of Al-Mg-Si-Cu alloy used for automotive panel. In addition, the paint-bake response of 6022 alloy with 0.3% Cu is compared to that of 6022 alloy.

2 Experimental

The alloys were prepared using high pure aluminum (99.9% Al), high pure magnesium (99.99% Mg), pure zinc (99.9% Zn), master alloys of Al-20% Si, Al-50%Cu, Al-10%Mn and Al-5%Cr (mass fraction). These raw materials were weighed precisely and melted in an electric

resistance crucible furnace, and then cast into an ingot (500 mm×115 mm×30 mm) in the water-cooling copper mould. The chemical compositions of the alloys are listed in Table 1. Two-stage homogenization treatment was performed at 425 °C for 10 h, then 550 °C for 8 h. The hot-rolled plate was cooled to room temperature followed by annealing at 550 °C for 1 h, then it was cold-rolled to a thin sheet of 1.0 mm. The cold-rolled plate was solutionised at 550 °C for 1 h, followed by water quenching, and then held at room temperature for 30 d (T4). Paint-bake treatment was conducted at 175 °C for 30 min (T8X).

Table 1 Chemical compositions of experimental alloys (mass fraction, %)

Alloy	Mg	Si	Cu	Fe
A(6022)	0.46	1.20	0.01	0.11
B(6022+Cu)	0.44	1.15	0.30	0.11
Alloy	Mn	Cr	Zn	Al
A(6022)	0.04	0.03	0.02	Bal.
B(6022+Cu)	0.07	0.04	0.02	Bal.

The microstructure was examined using a NIKON 200 optical microscope(OM) and a JSM 6480 SEM respectively. The composition analysis of the phases was performed by a GENESIS 7000 energy spectrometer coupled with the SEM, and the EDS results of the intermetallic compounds were corrected by ZAF (atomic number, absorption, fluorescence factors correction) method. The tensile properties were tested on a CSS 44100 tensile machine before and after paint-bake treatments (in T4/T4P and T8X tempers, respectively). Differential scanning calorimetry(DSC) analysis was performed in a NETZSCH STA 449C. During DSC measurement, samples were protected with flowing argon. The TEM samples were prepared by grinding the slices to a thickness of about 100 μm, then by twin-jet electropolishing using a 33% nitric acid-methanol solution at -20 °C. The foils were examined in an AJEM 2010 transmission electron microscope operated at 200 kV.

3 Results and discussion

3.1 As-cast microstructure

The as-cast microstructure of alloy B presents a typical dendrite network structure. It can be observed from Fig.1 that the phase constituents show irregular shapes such as plate and particle.

Fig.2 shows the SEM micrographs of phases of the as-cast alloy B. The EDS analyses indicate that the spherical particles are Al₂Cu (as shown in Fig.2(a)), and the mole ratio of Cu/Al is 1.8–2.5. Besides Al₂Cu phase, another Cu containing phase Q (Al₅Cu₂Mg₈Si₆) is

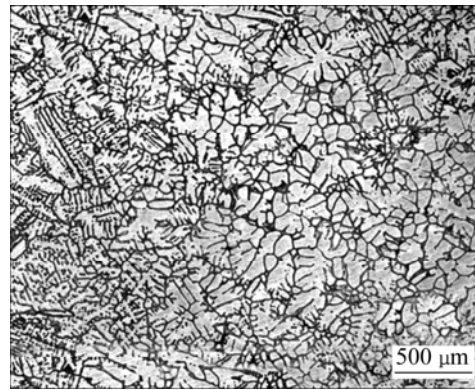


Fig.1 As-cast microstructure of alloy B

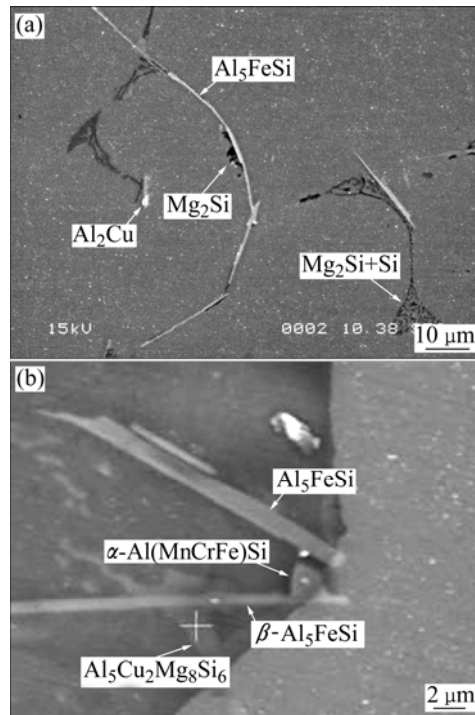


Fig.2 SEM micrographs of alloy B

observed. It can be seen from Fig.2 that Mg₂Si is a plate-like or block-shaped phase, and Si particles often present as binary eutectic with Mg₂Si, as shown in Fig.2(a). Fe has a very low solid solubility in Al (maximum 0.05% at equilibrium)[12], and most of Fe in Al alloys form a wide variety of Fe-containing intermetallics such as Al₁₃Fe₄, α-Al₈Fe₂Si, Al₅FeSi, depending on the alloy composition and its solidification conditions. There exists in the as-cast microstructure an amount of rod-like Al₅FeSi, in which the content of Fe is 15.63% and that of Si is 25.14%. Besides Al₅FeSi, there exists also a few blocky α-Al(MnCrFe)Si[14], as indicated in Fig.2(b). The results of EDS analysis are summarized in Table 2, together with the results obtained by former studies.

Table 2 Composition of Al_5FeSi and $\text{Al}_5\text{Cu}_2\text{Mg}_8\text{Si}_6$ phases (mass fraction, %)

Phase	Mg	Si	Fe	Cu	Ref.
Al_5FeSi		27.75	14.59		[13]
		25.14	15.63		Present work
$\text{Al}_5\text{Cu}_2\text{Mg}_8\text{Si}_6$	33	19.2		32.1	[14]
	29.22	15.2		26.9	Present work

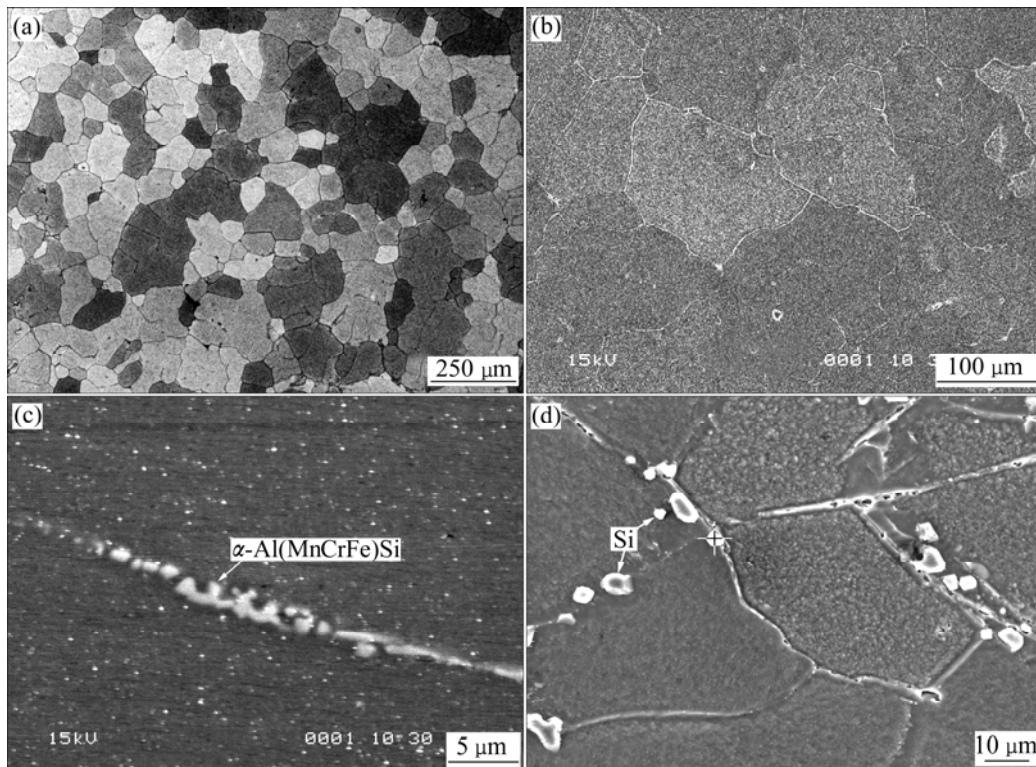
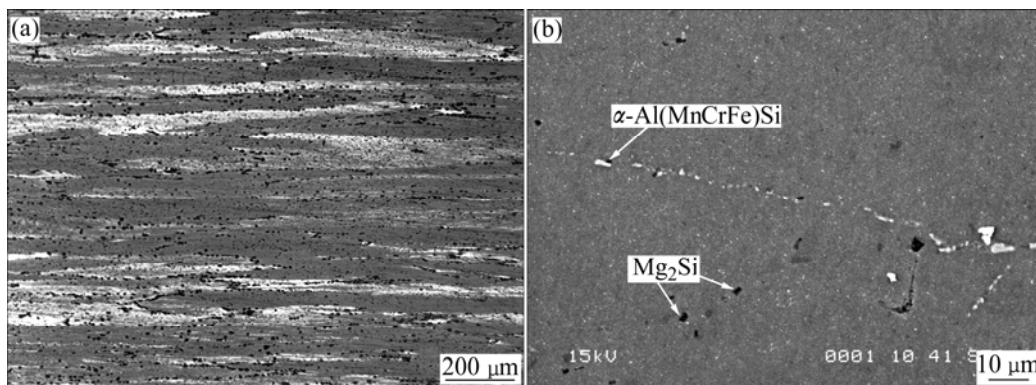
3.2 Homogenization

Fig.3 shows the OM and SEM micrographs of the homogenized alloy B. By comparing Figs.3(a) and (b) with Fig.1, it can be seen that the dendritic network formed during the cast disappears. SEM-EDS analyses

show that most of the Al_2Cu , Q and Mg_2Si phases are dissolved. Plate-like Si with the size of 2–8 μm locates near the grain boundaries, as shown in Fig.3(d). Most of the rod-like $\beta\text{-Al}_5\text{FeSi}$ phases transform into the strings of spherical $\alpha\text{-Al}(\text{MnCrFe})\text{Si}$ particles [13–14], as shown in Fig.3(c).

3.3 Microstructure after hot rolling

After hot rolling, the microstructure presents highly elongated grains, as shown in Fig.4(a), and the deformed microstructure is non-uniform. The phase constituents are almost unaffected by hot rolling, but secondary particles with the order of several micrometers are formed. These secondary particles include small $\alpha\text{-Al}(\text{Fe,Mn})\text{Si}$ precipitates with the size of 50 nm to

**Fig.3** Optical (a) and SEM (b, c, d) micrographs of homogenized alloy B**Fig.4** Microstructures of hot rolled alloy B (a) and precipitates after hot rolling (b)

several micrometers. Excessive Si particles with the size of several micrometers and Mg₂Si precipitates with the size up to 1 μm can also be observed, as shown in Fig.4(b). In contrast to the primary constituents shown in Fig.2, some of the secondary particles, especially Mg₂Si, can be re-dissolved during the further thermomechanical treatment. Accordingly, the size and dispersion of the secondary phases strongly depend on the conditions of the thermomechanical processing. Furthermore, Cu containing phases are not found in the deformed microstructure of alloy B. The precipitation of Mg₂Si particles during thermo- mechanical processing changes the Mg, Si super saturation in the matrix, and thus influences the formation of strengthening phases during aging treatment, especially β'' phase. The effect of thermomechanical processing conditions on the precipitation behavior of the strengthening phases especially β should be further investigated.

3.4 Paint-bake response

Before stamping, the plates in T4 temper are required to have low yield strength (preferably less than 140 MPa) for low spring-back and high formability (>24%) for obtaining complex automotive panels with high accuracy[9], and a relatively high yield strength (no less than 160 MPa) is required after paint-baking for in-service dent resistance. As listed in Table 3, alloys A and B all meet these requirements, and the Cu addition significantly increases the aged strength of plate. Whilst, the paint-bake response (PBR) is remarkably enhanced by increasing Cu content, as shown in Fig.5. This indicates that the Cu addition is favorable for paint-bake cycle of the alloy.

Table 3 Mechanical properties of alloys in T4 and T8X conditions

Alloy and temper	R _{p0.2} /MPa	R _m /MPa	A/%
Alloy A in T4 condition	131	271	33.2
Alloy B in T4 condition	135	280	32.8
Alloy A in T8X condition	162	276	26.5
Alloy B in T8X condition	176	295	24.2

To characterize the precipitation state of Mg₂Si phase before and after bake cycle and understand the mechanism of the Cu addition on the paint-bake cycle, DSC and TEM experiments were employed in this work. Fig.6 shows the bright-field TEM images of alloy B in T4 condition. No distinct features of pre-β precipitates are observed in Fig.6(a). However, some Al, Fe, Mn, Si containing phases are observed as shown in Fig.6(b). Pre-β precipitates have not been observed in alloy A-T4.

After paint-bake treatment, some dot-like pre-

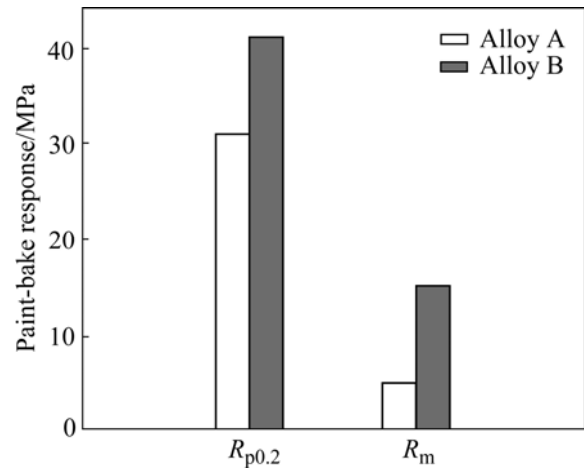


Fig.5 Paint-bake response (PBR) of studied alloys

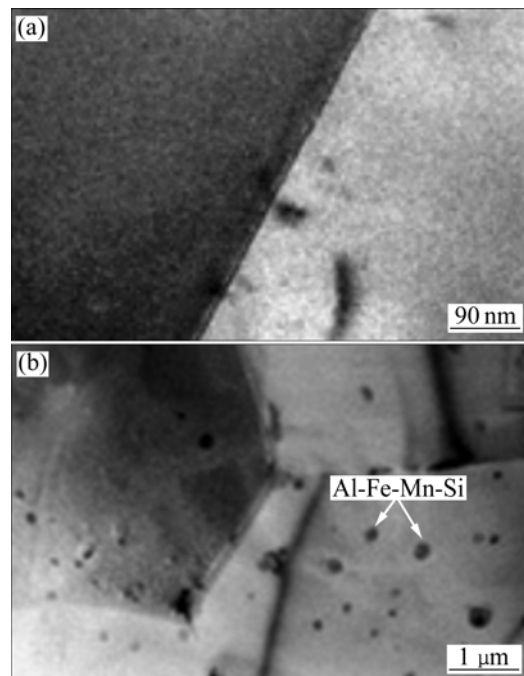


Fig.6 TEM images of alloy B in T4 state

cipitates are observed in alloy B-T8X, as shown in Fig.7(a). According to the work of MURAYAMA et al[15], these precipitates should be β'' phase. Furthermore, some Al and Cu containing phases are observed after paint-bake, as indicated in Fig.7(b). TEM-EDX results suggest those phases are θ phases or the precursor of θ phases (the Cu/Al molar ratio being about 2). Thus, it could be concluded that β'' and precursor of θ phase are formed in T8X condition of 6022 alloy with 0.3% Cu. This finding is different from the result obtained by MIAO et al[10], who reported that β'' and precursor of θ phase were not observed in 6022 alloy with 0.91% Cu after paint-bake treatment. But GUPTA et al[11] proposed that an addition of Cu ≥ 0.25% will induce the precipitation of additional pre-

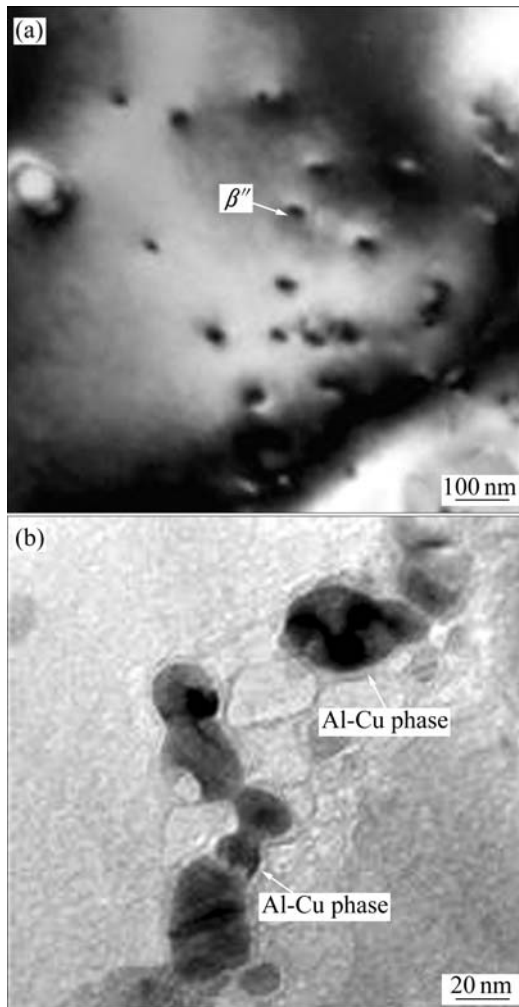


Fig.7 Morphologies of β'' (a) and precursor of θ (b) in T8X state experimental alloy

cursors of the CuAl_2 phase during paint-bake cycle. GUPTA et al[11] further proposed that the precipitation process of strengthening phases is dependant not only on alloy composition but also on processing conditions. Meanwhile, β'' phase was not found in alloy A-T8X. This is consistent with the report of MORLEY et al[16] and MIAO et al[10]. Therefore, it can be concluded that Cu addition enhances the formation of β'' during paint-bake cycle, which is further confirmed by DSC experiments.

Fig.8 shows the formation peak of β'' in as-quenched samples of the alloys A and B, and the peak temperatures are listed in Table 4. From the DSC curves, a clear difference can be observed about β'' formation in alloys A and B. β'' forming in alloy B is slightly earlier than that in alloy A and shows a much higher potential in strengthening, which indicates that copper facilitates the formation of β'' during paint-bake cycling. Meanwhile, it can also be found that the peak reaction temperatures (Table 4) for β'' formation shift to lower temperatures,

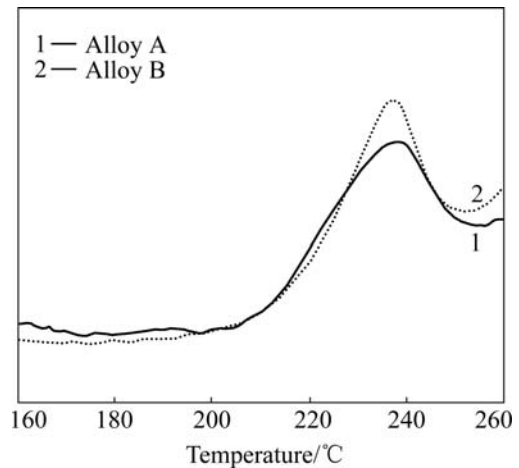


Fig.8 DSC curves of as-quenched samples

Table 4 DSC peak temperature ($^{\circ}\text{C}$) for β'' formation in Fig.8

Heating rate/ $(^{\circ}\text{C}\cdot\text{min}^{-1})$	Alloy A	Alloy B
5	239.1	236.2

further indicating the easy formation of β'' , and thus a faster rate of formation of β'' phase owing to Cu additions.

4 Conclusions

1) The main phases in the as-cast microstructure of 6022 alloy with 0.3% Cu are Mg_2Si , Si, $\text{Al}_5\text{Cu}_2\text{Mg}_8\text{Si}_6$ (Q), Al_5FeSi , $\alpha\text{-Al}(\text{MnCrFe})\text{Si}$ and CuAl_2 . During the homogenization process, most of Al_2Cu , Q and Mg_2Si are dissolved, and plate-like Al_5FeSi particles are transformed into multiple, spherical $\alpha\text{-Al}(\text{MnCrFe})\text{Si}$ particles. After deformation processing, the phase constituents in the alloy change less, except the precipitation of Mg_2Si .

2) Cu addition increases the paint-bake response of the 6022 alloy by facilitating the formation of β'' phase. Therefore, the strength of 6022 alloy with certain Cu addition is higher than that of 6022 alloy without Cu after paint-bake cycle.

References

- [1] ENGLER O, HIRSCH J. Texture control by thermomechanical processing of AA6xxx Al-Mg-Si sheet alloys for automotive applications—A review [J]. *Materials Science and Engineering A*, 2002, 336: 249–262.
- [2] SONG Y, CROSS M D J, RAINFORTH W M, WYNNE B P. Observations of strain induced precipitation during the thermomechanical processing of AA6111 alloy [J]. *Materials Science Forum*, 2007, 550: 211–216.
- [3] BIROL Y. Pre-aging to improve bake hardening in a twin-roll cast Al-Mg-Si alloy [J]. *Materials Science and Engineering A*, 2005, 391:

- 175–180.
- [4] KAMAT R G, BUTLER J F, MURTHA S J, BOVARD F S. Alloy 6022-T4E29 for automotive sheet applications [J]. *Materials Science Forum*, 2002, 396/402: 1591–1596.
- [5] QUAINOO G K, YANNACOPOULOS S. The effect of cold work on the precipitation kinetics of AA6111 aluminum [J]. *Journal of Materials Science*, 2004, 39: 6495–6502.
- [6] GUPTA A K, LLOYD D J, COURT S A. Precipitation hardening processes in an Al-0.4%Mg-1.3%Si-0.25%Fe aluminum alloy [J]. *Materials Science and Engineering A*, 2001, 301: 140–146.
- [7] CHEN S P, MUSSERT K M, ZWAAG S V D. Precipitation kinetics in Al6061 and in an Al6061-alumina particle composite [J]. *Journal of Materials Science*, 1998, 33: 4477–4483.
- [8] MARIOARA C D, ANDERSEN S J, JANSEN J, ZANDBERGEN H W. The influence of temperature and storage time at RT on nucleation of the β'' phase in a 6082 Al-Mg-Si alloy [J]. *Acta Materialia*, 2003, 51: 789–796.
- [9] JANSE J E, ZHUANG L, MOOI J, SMET D. Evaluation of effect of Cu on the paint-bake response of presaged AA6xxx [J]. *Materials Science Forum*, 2002, 396/402: 607–612.
- [10] MIAO W F, LAUGHLIN D E. Effects of Cu content and preaging on precipitation characteristics in aluminum alloy 6022 [J]. *Metallurgical Materials Transactions A*, 2000, 31: 361–371.
- [11] GUPTA A K, MAROIS P H, LLOYD D J. Study of the precipitation kinetics in a 6000 series automotive sheet material [J]. *Materials Science Forum*, 1996, 217/222: 801–808.
- [12] MONDOLFO L F. Aluminum alloys: structure and properties [M]. WANG Z T, transl. Beijing: Metallurgical Industry Press, 1988: 702. (in Chinese)
- [13] KUIJPERS N C W, VERMOLEN F J, VUIK C, KOENIS P T G, NILSEN K E, VAN D Z S. The dependence of the β -AlFeSi to α -Al(FeMn)Si transformation kinetics in Al-Mg-Si alloys on the alloying elements [J]. *Materials Science and Engineering A*, 2005, 394: 9–19.
- [14] LODGAARD L, RYUM N. Precipitation of dispersoids containing Mn and/or Cr in Al-Mg-Si alloys [J]. *Materials Science and Engineering A*, 2000, 283: 144–152.
- [15] MURAYAMA M, HONO K, MIAO M F, LAUGHLIN D E. The effect of Cu additions on the precipitation kinetics in an Al-Mg-Si alloy with excess Si [J]. *Metallurgical and Materials Transactions A*, 2001, 32: 239–246.
- [16] MORLEY A I, ZANDBERGEN M W, CERESO A, SMITH G D W. The effect of pre-aging and addition of copper on the precipitation behavior of Al-Mg-Si alloys [J]. *Materials Science Forum*, 2006, 519/521: 543–548.

(Edited by YUAN Sai-qian)